https://doi.org/10.20965/jrm.2020.p0297

Paper:

Tactile Sensor with High-Density Microcantilever and Multiple PDMS Bumps for Contact Detection

Tomoya Fujihashi, Fumitoshi Suga, Ryoma Araki, Jyun Kido, Takashi Abe, and Masayuki Sohgawa

Niigata University
8050 Ikarashi 2-no-cho, Nishi-ku, Niigata 950-2181, Japan
E-mail: sohgawa@eng.niigata-u.ac.jp
[Received October 27, 2019; accepted March 18, 2020]

In the study, we investigated a detection method of partial contact of an object owing to curved or uneven surface of the contact object by a tactile sensor. The sensor is developed using three microcantilevers embedded in a polydimethylsiloxane (PDMS) bump. First, three bumps were employed to place a bump for each cantilever. It was possible to detect a contact position because the resistance change in the strain gauge on the cantilever under each bump significantly depended on the contact/non-contact state of each bump. Second, a tactile sensor with high-density arrangement of microcantilevers was used to detect partial or tilted contact situations. The results indicated that the output of a tactile sensor with high-density arrangement of microcantilevers reflected partial or tilted contact. It is suggested that a tactile sensor with multiple bumps and high-density microcantilevers allows for more dexterous gripping control based on the shape of the object and contact angle.

Keywords: tactile sensor, microcantilever, PDMS bumps, contact detection, gripping control

1. Introduction

The introduction of robots in various fields to perform work previously done by humans is expected in areas such as agriculture, nursing-care, and housework [1]. When robots work instead of humans, it is assumed that the robots will perform contact, operation, and gripping of objects of various shapes. Robots can easily grip rigid and definite shaped objects. However, they are unable to grip flexible, soft, and indefinite-shaped objects. To grip them, recognition of shape, hardness, and deformation of the object is required [2, 3]. Furthermore, proximity and slipping detection is also important in dexterously gripping soft or fragile objects without deformation and damage [4–6]. Therefore, tactile sensors are essential to recognize these properties. Various types of tactile sensors are proposed and developed [1–3]. Nevertheless, they are not fully utilized in practical terms owing to their size or cost.

In previous studies, we developed tactile sensors with microcantilevers fabricated by micro-electromechanical systems (MEMS) technologies embedded in polydimethylsiloxane (PDMS) [7–12]. The sensor can detect normal and shear forces. Furthermore, it exhibits sensitivity to light and allows optical proximity sensing [13–15]. We already constructed a grasping control system using a proximity and tactile combination MEMS sensor with a PDMS bump [16, 17]. The tactile sensor is small (chip size: 5 mm $\times$ 5 mm) and its cost is expected to reduce by mass production. It is demonstrated that soft objects can be successfully gripped with small deformation using the system. However, in previous studies, the object shape was definite, and its variation was not considered. In actual conditions, partial contact occurs given object shapes with curved or uneven surfaces.

In the study, we examined the detection method of partial contact by two methods. First, we proposed and fabricated a tactile sensor with multiple PDMS bumps to place a bump for each microcantilever. The study investigated detecting partial contact with each bump from response of the microcantilever under each bump. The second method corresponds to a higher arrangement of microcantilevers. Recently, we successfully developed a tactile sensor with microcantilevers that are smaller than sensors in previous studies and arranged at a higher density [18]. The results indicated that the accurate direction of lateral deformation by the applied force is obtained by the output distribution from high-density microcantilevers. Thus, we attempted to detect partial and tilted contact by lateral deformation of PDMS from the contact point to the surrounding direction by using a tactile sensor with high-density microcantilevers. In the study, the effectiveness of each approach for partial contact detection is evaluated independently to present guidelines for a fusion of design of two approaches in the future.

2. Tactile Sensor with Multiple Bumps and Detection Principle

Figure 1 shows a chip of proximity and tactile sensor with three PDMS bumps as a contact part. Three can-

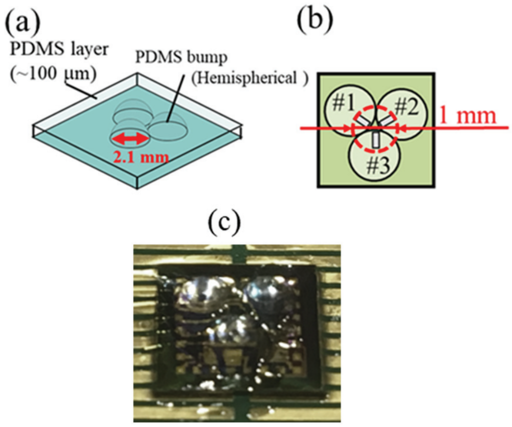

Fig. 1. Tactile sensor with microcantilevers with three PDMS bumps: (a) schematic view, (b) positional relation between microcantilevers and bumps, and (c) photograph of the fabricated sensor.

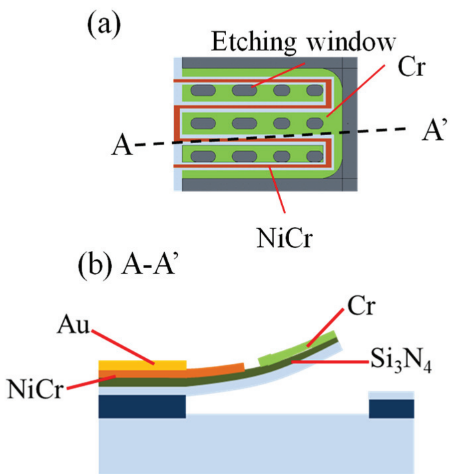

Fig. 2. (a) Top view and (b) cross-sectional (A-A') view of the microcantilever.

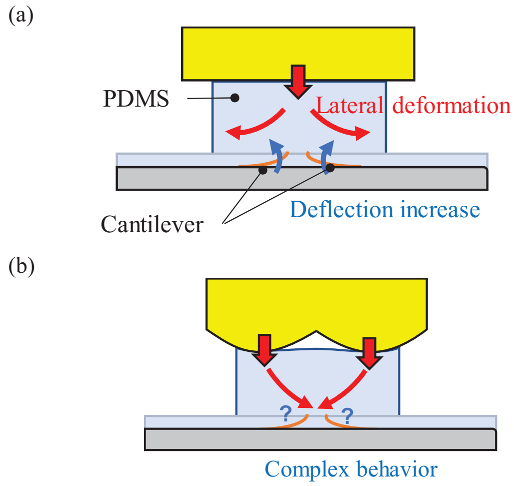

Fig. 3. Schematic illustrations of lateral deformation of a cylindrical PDMS bump employed in previous studies and behavior of the microcantilevers when normal force is applied in the case of contact with (a) flat- and (b) uneven-surfaced objects.

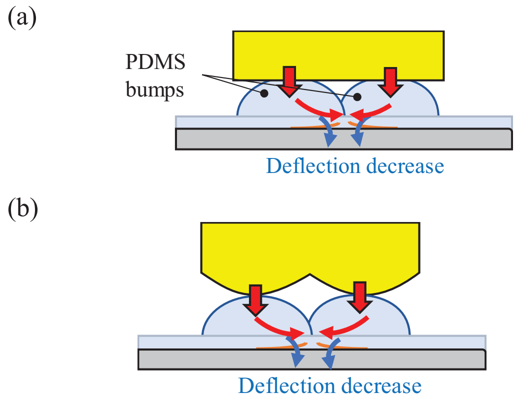

Fig. 4. Schematic illustrations of lateral deformation of multiple PDMS bumps employed in the study and behavior of the microcantilevers when normal force is applied in the case of contact with (a) flat- and (b) uneven-surfaced objects.

tilevers with a length of 290 μm and a width of 200 μm are arranged inside a 1-mmϕ in a manner similar to sensors used in previous studies. They were embedded in thin PDMS layer. Subsequently, in an extant study, a cylindrical or hemispherical shaped PDMS bump was attached on three cantilevers [16, 17, 19]. Conversely, in the study, three PDMS bumps were attached to place a bump on each cantilever, as shown in **Fig. 1(b)**. The bump is hemispherical in shape and 2.1 mm in diameter. The sensor is expected to allow detection of the contact part in the case of a partial contact without design changes in the microcantilever arrangement in the sensor, as employed in previous studies, and with increases in the number of connections and output signals.

Figure 2 shows the top view and a cross-sectional view of the MEMS cantilever. The cantilever structure was fabricated by sacrificial etching of buried oxide layer of a silicon on insulator (SOI) wafer. Specifically, Si_3N_4, NiCr, Au, and Cr thin films were formed on the cantilever as insulating, strain gauge, wiring, and stress control layers, respectively. **Fig. 3(a)** shows the schematic illustration of behavior of microcantilevers embedded in PDMS when a normal force is applied to the PDMS bump in the case of the sensor with a cylindrical PDMS bump, as used in previous studies [16, 17]. Resistance change in the NiCr strain gauge layer with deflection change in the cantilever is measured as the output of the sensor. The PDMS deforms laterally with respect to the normal force as shown in **Fig. 3**, and thus the deflection of the cantilever increases and resistance of strain gauge decreases with increases in compressive strain. However, in the case of contact with an object which has uneven surface (as shown in **Fig. 3(b)**), deflection behavior of microcantilevers becomes more complex. On the other hand, **Fig. 4** shows the case of the sensor with a bump placed over each cantilever employed in the study. The deflection amount of microcantilevers decreases by the lateral

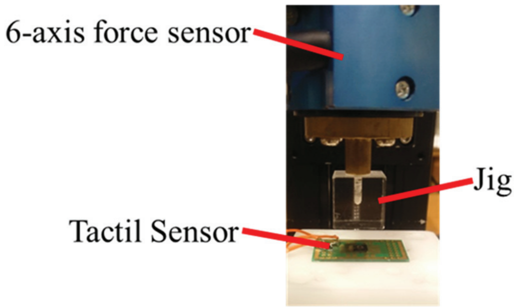

Fig. 5. Three-axis motorized stage with a reference force sensor for contact measurement.

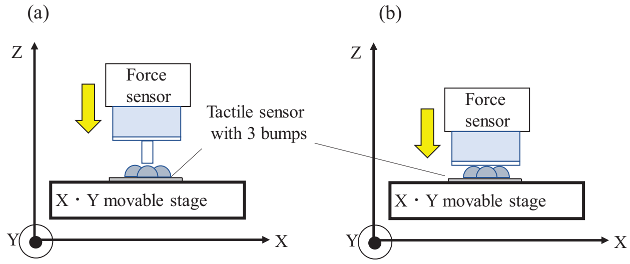

Fig. 6. Schematic illustration of contact measurement. Tactile sensor with three PDMS bumps pressed by (a) a jig which presses one of the bumps and (b) large object covering all three bumps.

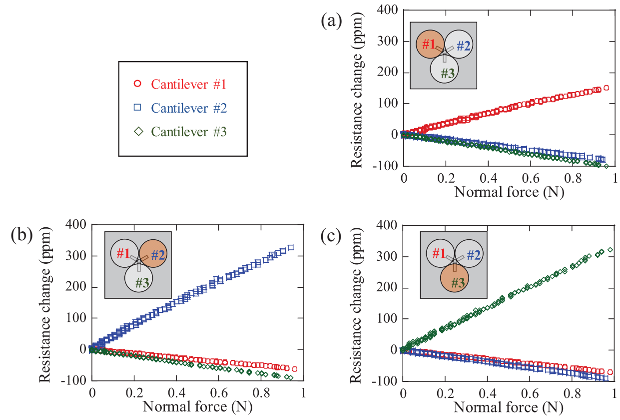

Fig. 7. Resistance change in strain gauge for each cantilever when normal force is applied to (a) bump #1, (b) #2, or (c) #3.

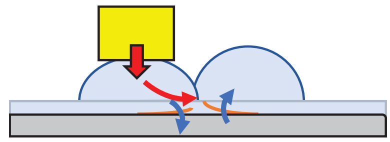

Fig. 8. Behavior model of cantilevers embedded under multiple bumps.

deformation of the PDMS bump because the tip direction of each microcantilever is from the center to the outside of the bump. For contact with an uneven-surfaced object, as shown in **Fig. 4(b)**, the behavior of microcantilevers is not extremely complex and is similar to that with a flat object because bumps over each cantilever are separated.

3. Contact Measurement Using Tactile Sensor with Multiple Bumps

Figure 5 shows a 3-axis motorized stage (SHOT-204MS, Sigma Koki) with a 6-axis force sensor (UFS2012A-05, Nitta), for reference, that is used to perform contact measurement with MEMS tactile sensors. **Fig. 6** shows a schematic illustration of the contact measurement. Initially, normal force of up to 0.5 N was applied to one of the PDMS bumps of the tactile sensor by using a jig with a square surface (1.5 mm × 1.5 mm). Additionally, the tactile sensor was pressed with a sufficiently large object covering all three PDMS bumps. Resistance change in the strain gauge on the cantilever was measured by a digital multimeter (R6581, ADCMT).

Figure 7 shows the resistance change in strain gauge on the three cantilevers when normal force is applied to each bump by assuming detection of a contact situation with only one bump. Sensitivity (slope of resistance change) of three cantilevers to the normal force is different and especially that of the cantilever under bump #2 is lower than other cantilevers. This appears owing to the variation in initial deflection between cantilevers. It is necessary to perform a correction based on sensitivity of each cantilever measured by resistance change by applying a known force in advance. Furthermore, the results indicate that the resistance for the cantilever under the force-applied bump increases linearly to the force. The cantilever deflection under each bump decreases as shown in **Fig. 8**, and thus resistance of the strain gauge increases. Conversely, the resistance under the bumps without the application of force exhibits a slight decrease. The result is considered to be due to lateral deformation propagation from the force-applied bump through the thin PDMS layer to the bottom of the other bumps, and this increases cantilever deflection as shown in **Fig. 8**.

Resistance change for each bump linearly increases when the normal force is applied to itself and decreases when the normal force is applied to other bumps. The result is expressed as follows:

$$\begin{pmatrix} S_1 \\ S_2 \\ S_3 \end{pmatrix} = \begin{pmatrix} k_{11} & -k_{21} & -k_{31} \\ -k_{12} & k_{22} & -k_{32} \\ -k_{13} & -k_{23} & k_{33} \end{pmatrix} \begin{pmatrix} F_1 \\ F_2 \\ F_3 \end{pmatrix}, \quad (1)$$

where S_i, k_{ij}, and F_i $(i, j = 1, 2, 3)$ denote sensor outputs (resistance change), sensitivities, and normal force applied to each bump, respectively. Eq. (1) is modified using inverse matrix of k_{ij} as follows:

$$\begin{pmatrix} F_1 \\ F_2 \\ F_3 \end{pmatrix} = \begin{pmatrix} k_{11} & -k_{21} & -k_{31} \\ -k_{12} & k_{22} & -k_{32} \\ -k_{13} & -k_{23} & k_{33} \end{pmatrix}^{-1} \begin{pmatrix} S_1 \\ S_2 \\ S_3 \end{pmatrix}, \quad (2)$$

Sensitivity matrix, k_{ij}, is experimentally determined in

Table 1. Sensitivity values for each cantilever to force applied to bumps.

Cantilever	Sensitivity (ppm/N)		
	F_1	F_2	F_3
#1	160	−83.5	−104
#2	−63.5	353	−95.2
#3	−71.1	−92.0	330

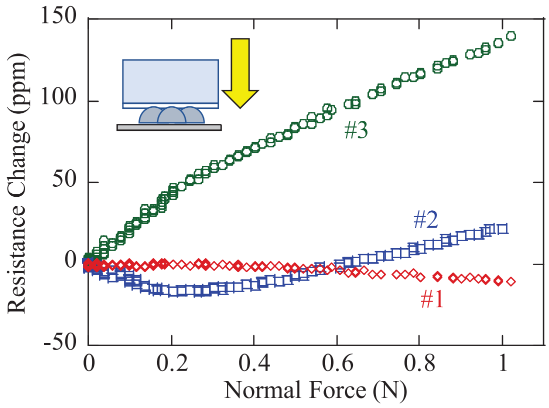

Fig. 9. Output of each cantilever when the sensor is pressed against a large object covering all bumps.

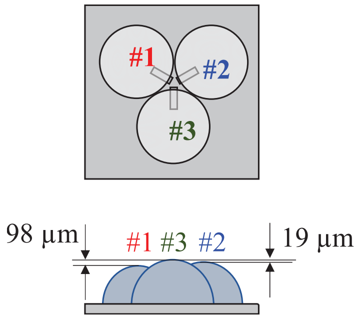

Fig. 10. Differences in the height of three bumps (as measured by a laser displacement meter).

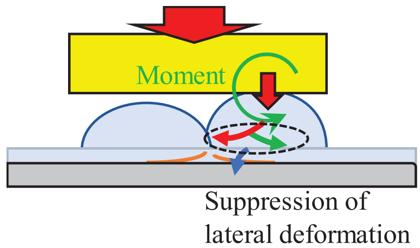

Fig. 11. Suppression of lateral deformation of PDMS due to the moment about the contact point by partial contact.

advance by the measurement result. **Table 1** shows k_{ij} values as obtained by linear regression of data in **Fig. 7**. Normal force is calculated from the values and sensor output using Eq. (2). Based on the measurement, the results indicate that the bump that contacts the object can be discriminated and the applied normal force due to contact can be detected by the tactile sensor with multiple bumps.

Figure 9 shows the change in resistance for three cantilevers when the sensor is pressed with the object covering all bumps, assuming a contact situation with multiple bumps simultaneously. The tendency of resistance of each cantilever to normal force is different. This is considered to be caused by the slight variation in heights of the three bumps due to the variation in the mold size or thickness of adhesive layer, as shown in **Fig. 10**. The cantilever is arranged under the highest bump #3 that first contacts the object, and thus the resistance monotonically increases when the normal force increases, as shown in **Fig. 7(c)**. However, the resistance change for bump #3 is slightly lower than that in the case of **Fig. 7(c)**. Furthermore, the resistance of cantilever under bump #1 does not exhibit a significant change in contrast to **Fig. 7(c)**. Although the exact cause is unknown, partial contact can lead to a moment about the contact point, and this suppresses lateral deformation of PDMS, as shown in **Fig. 11**. Conversely, the resistance change for the cantilever arranged under the next highest bump #2 stops decreasing and begins increasing at approximately 0.2 N. Concurrently, the increasing rate of resistance for the cantilever #3 decreases. This indicates that the object is in contact with the second height bump at approximately 0.2 N. The resistance change for cantilever arranged under the lowest bump #1 exhibits a slightly monotonical decrease, as shown in **Fig. 7(b)** or **(c)**, because it does not contact the object in this measurement. It is suggested that slight difference of bump height significantly affects the resistance change for each cantilever, and thus bumps should be formed with uniformity by using an accurate mold or uniform adhesive. If the bumps are formed with same height, then it is estimated as to which bump is contact with the object. Therefore, the results indicate that it is possible to discriminate between contact and non-contact and estimate applied normal force to each bump by using the tactile sensor with same height multiple bumps and also in the case of contact with multiple bumps.

4. Contact Measurement Using Tactile Sensor with High-Density Microcantilevers

It is considered that insufficient spatial resolution can exist with three cantilevers for detecting contact status on objects with more complex surface shapes. Therefore, we developed a tactile sensor with further miniaturized and high-density microcantilevers as shown in **Fig. 12** [18]. The size of the cantilever includes 155 μm in length and 70 μm in width. A total of 12 cantilevers are arranged in a 1 mmϕ, and the density of cantilevers is thrice that of the sensor with three cantilevers. To remove the effect of surface shape of the sensor, a cylindrical PDMS bump with a flat surface similar to that in previous studies was employed. In an extant study [18], the basic response of the sensor to applied force was characterized, and it was

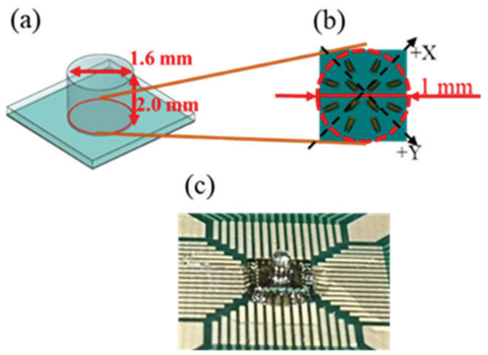

Fig. 12. Schematic illustration of tactile sensor with high-density microcantilevers: (a) cylindrical PDMS bump, (b) arrangement of cantilever (length: 155 μm, width: 70 μm), and (c) photograph of the fabricated sensor.

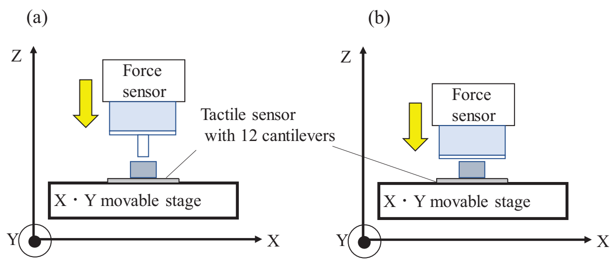

Fig. 13. Schematic illustration of contact measurement of tactile sensor with 12 cantilevers pressed by objects with (a) small or (b) large surface area.

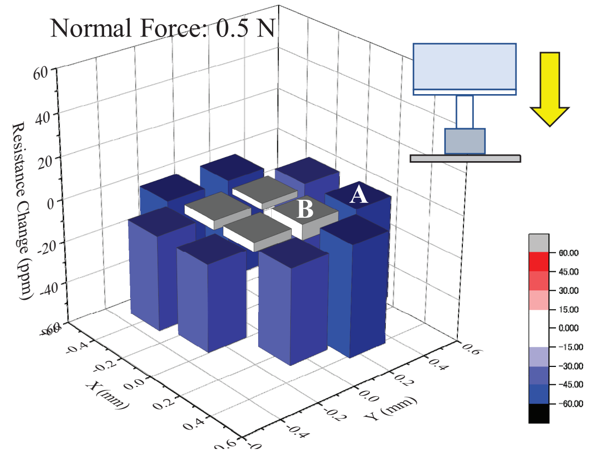

Fig. 14. Relationship between resistance change and position for 12 cantilevers in tactile sensor pressed by an object with small surface area (0.5 mmϕ).

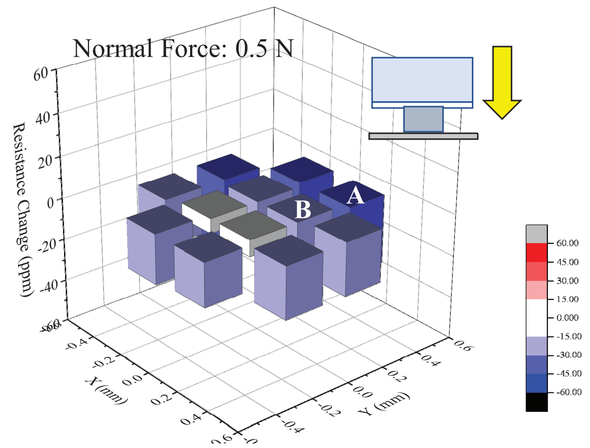

Fig. 15. Relationship between resistance change and position for 12 cantilevers in the tactile sensor pressed by an object with high surface area (20 × 20 mm).

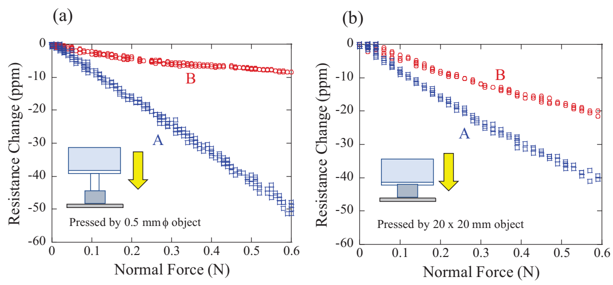

Fig. 16. Resistance change as a function of normal force for cantilevers arranged in external (A) and internal (B) sides when the bump is pressed by (a) small or (b) large objects.

demonstrated accurate direction shear force was detected. However, responses in the case of partial and tilted contact are not characterized. Hence, in the study, we assume partial contact situations, and a tactile sensor with 12 cantilevers was pressed by objects with surface area lower (0.5 mmϕ) or higher (20 × 20 mm) than that of cylindrical bump as shown in **Fig. 13**.

Figures 14 and **15** show the relationship between resistance change and position for 12 cantilevers in tactile sensor when a normal force of 0.5 N is applied by an object with surface area lower and higher than that of tactile sensor bump, respectively. Resistance for cantilevers arranged at external side decreases and that for those arranged at internal side exhibit a slight decrease in the case of contact with small objects. Conversely, in the case of a large object covering the entire surface of the bump, although a similar tendency is observed, the difference in resistance change between external and internal side cantilevers is not high. Additionally, resistance change for external side cantilevers arranged at lower Y-value position is slightly lower than that arranged at higher Y-value position. If there is a possibility that flat bump surface of the sensor is not perfectly parallel to surface of the object with large surface area, then it is considered that contact with slight tilting leads to this type of bias in sensitivity. **Fig. 16** shows resistance change as a function of normal force for cantilevers arranged at external and internal sides (shown as A and B in **Figs. 14** and **15**) when the bump is pressed by the object with (a) small or (b) large surface area. The results indicate that difference in resistance change to normal force between A and B is evidently higher in the case of the small object (**Fig. 16(a)**).

To confirm the behaviors of the cantilever, deformation

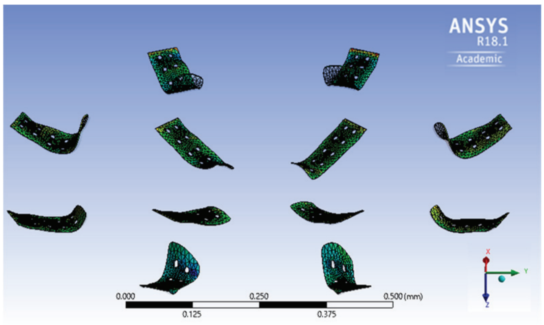

Fig. 17. FEM analysis result of deformation shape of cantilevers embedded in PDMS bump when the bump is pressed by a large object.

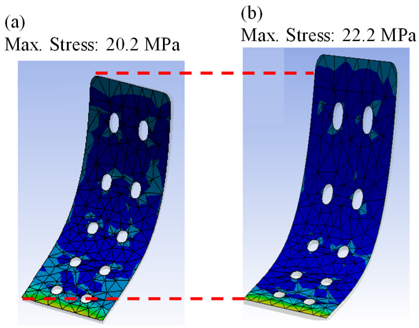

Fig. 18. FEM analysis results of stress distribution for the cantilever arranged at the internal side when the bump is pressed by (a) small or (b) large objects.

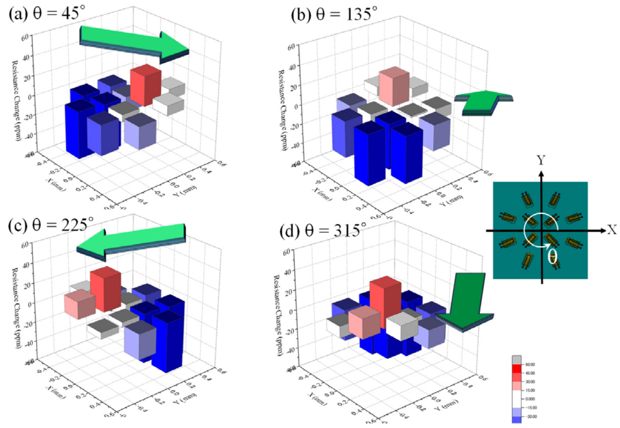

Fig. 19. Resistance change in the case of contact with normal force of 0.5 N and tilt angle of 10° at (a) $\theta = 45°$, (b) $\theta = 135°$, (c) $\theta = 225°$, and (d) $\theta = 315°$.

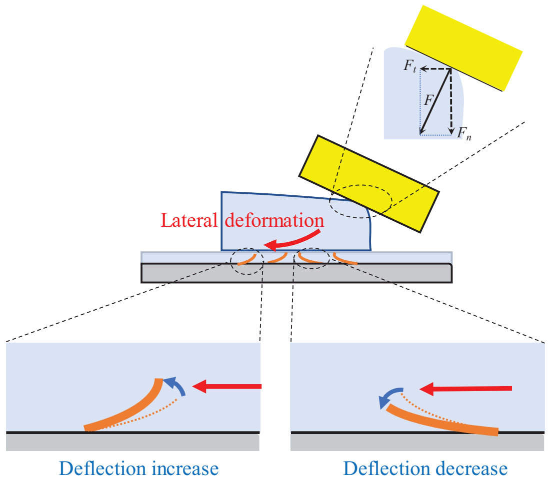

Fig. 20. Schematic illustration of lateral deformation induced by tilting contact.

of cantilever with applying force was analyzed by finite element method (FEM) using ANSYS (R18.1). **Fig. 17** shows the analysis result of deformation shape (enlarged) of cantilevers embedded in PDMS bump pressed by the object with higher surface area. Deflection increase in cantilevers arranged at the external side evidently exceeds that of cantilevers arranged at the internal side. This is because lateral deformation of PDMS increases closer to the exterior edge of the bump. **Fig. 18** shows the calculated distribution of the first principal stress at the surface of the cantilever arranged at internal side when the bump is pressed by a small or large object. The deformation amount of the cantilever tip and the maximum value of stress in the case involving pressing by the small object (**Fig. 18(a)**) are lower than that in the case of large object (**Fig. 18(b)**). This indicates that the difference between resistance change shown in **Figs. 14–16** is due to the behavior of cantilever deformation embedded under the bump.

In addition, resistance change for 12 cantilevers was also measured when the large object contacts the bump of tactile sensor with tilting. **Fig. 19** shows resistance change in the case of contact with normal force corresponding to 0.5 N and tilt angle corresponding to 10° in various direction (θ). The results indicate that resistance for cantilevers arranged at near contact point in tilting direction increases. On the other hand, resistance arranged at an opposite side of contact point decreases. **Fig. 20** shows a schematic illustration of PDMS deformation and deflection behavior of cantilevers in the case of tilting contact. At the contact point, contact force is applied in oblique direction to PDMS surface. Thus, applied contact force includes both normal (F_n) and tangential (F_t) components to the PDMS surface. Specifically, the PDMS deforms laterally from contact point to the other side with respect to the normal force. Furthermore, PDMS is deformed laterally by tangential force in the same direction. The direction of the tip of cantilevers arranged at near contact point is parallel to lateral deformation of the PDMS while that of cantilevers arranged at an opposite side is antiparallel. Hence, deflection of the cantilever arranged at the contact point increases and that arranged at the other side decreases. This implies that tilting contact and its direction can be assumed from spatial distribution of changes in resistances for 12 cantilevers.

The results revealed from the output of 12 cantilevers depend on contact area of the object and tilting contact. If this sensor is installed on a robotic hand and machine learning is performed in advance on the correlation between the output distribution from the 12 cantilevers and the contact parameters, such as the contact angle and area, then it is possible to dexterously control gripping state of the robotic hand based on the inverse estimation of the contact parameters from the sensor output.

5. Conclusions

The results of the study indicated that various contact conditions can be detected by a sensitive MEMS tactile sensor with multiple PDMS bumps or high-density microcantilevers. The employment of multiple PDMS bumps enables detection of a contact position because resistance change in strain gauge on the cantilever under each bump significantly depends on contact/non-contact state of bumps. Furthermore, it is demonstrated that output distribution from tactile sensor with 12 cantilevers depends on partial and tilted contact situations. In a future study, we will develop a tactile sensor by combining multiple bumps and high-density cantilevers. Furthermore, we will demonstrate gripping of soft or indefinite shaped objects, such as gel and tissue, by a robotic hand with control through tactile and proximity information.

Acknowledgements

A part of the study was supported by JSPS KAKENHI Grant Number JP15H02230, JP17K17737, JP18H03314, and JP19K04290 and Adaptable and Seamless Technology Transfer Program through Target-driven R&D (A-STEP) from Japan Science and Technology Agency (JST).

References:

[1] R. S. Dahiya, G. Metta, M. Valle, and G. Sandini, "Tactile Sensing – From Humans to Humanoids," IEEE Trans. Robot., Vol.26, No.1, pp. 1-20, doi:10.1109/TRO.2009.2033627, 2010.

[2] Z. Kappassov, J.-A. Corrales, and V. Perdereau, "Tactile sensing in dexterous robot hands – Review," Rob. Auton. Syst., Vol.74, pp. 195-220, doi:10.1016/j.robot.2015.07.015, 2015.

[3] H. Yousef, M. Boukallel, and K. Althoefer, "Tactile sensing for dexterous in-hand manipulation in robotics – A review," Sens. Actuators, A Phys., Vol.167, No.2, pp. 171-187, doi:10.1016/j.sna.2011.02.038, 2011.

[4] D. Yamada, T. Maeno, and Y. Yamada, "Artificial finger skin having ridges and distributed tactile sensors used for grasp force control," J. Robot. Mechatron., Vol.14, No.2, pp. 140-146, doi:10.20965/jrm.2002.p0140, 2002.

[5] S. Teshigawara, T. Tsutsumi, Y. Suzuki, and M. Shimojo, "High speed and high sensitivity slip sensor for dexterous grasping," J. Robot. Mechatron., Vol.24, No.2, pp. 298-310, doi:10.20965/jrm.2012.p0298, 2012.

[6] Y. Mizoguchi, K. Tadakuma, H. Hasegawa, A. Ming, M. Ishikawa, and M. Shimojo, "Development of Intelligent Robot Hand Using Proximity, Contact and Slip Sensing," Trans. Soc. Instrum. Control Eng., Vol.46, No.10, pp. 632-640, doi:10.9746/sicetr.46.632, 2010 (in Japanese).

[7] M. Sohgawa, T. Mima, H. Onishi, T. Kanashima, M. Okuyama, K. Yamashita, M. Noda, M. Higuchi, and H. Noma, "Tactile array sensor with inclined chromium/silicon piezoresistive cantilevers embedded in elastomer," Proc. of Transducers 2009, pp. 284-287, doi:10.1109/SENSOR.2009.5285509, 2009.

[8] H. Tachibana, S. Kamanaru, T. Mima, M. Sohgawa, T. Kanashima, K. Yamashita, M. Noda, M. Okuyama, H. Noma, and M. Higuchi, "Fabrication and Basic Characteristics of Multiaxial Tactile Sensor with 3 Cantilevers," IEEJ Trans. Sens. Micromachines, Vol.130, No.6, pp. 223-229, doi:10.1541/ieejsmas.130.223, 2010 (in Japanese).

[9] M. Sohgawa, T. Uematsu, W. Mito, T. Kanashima, M. Okuyama, and H. Noma, "Crosstalk Reduction of Tactile Sensor Array with Projected Cylindrical Elastomer over Sensing Element," Jpn. J. Appl. Phys., Vol.50, No.6, 06GM08, doi:10.1143/JJAP.50.06GM08, 2011.

[10] D. Hirashima, T. Uematsu, M. Sohgawa, W. Mito, T. Kanashima, M. Okuyama, and H. Noma, "Fabrication of a Flexible Array for Tactile Sensors with Microcantilevers and the Measurement of the Distribution of Normal and Shear Forces," Jpn. J. Appl. Phys., Vol.50, No.6, 06GM02, doi:10.1143/JJAP.50.06GM02, 2011.

[11] M. Sohgawa, D. Hirashima, Y. Moriguchi, T. Uematsu, W. Mito, T. Kanashima, M. Okuyama, and H. Noma, "Tactile sensor array using microcantilever with nickel-chromium alloy thin film of low temperature coefficient of resistance and its application to slippage detection," Sens. Actuators A, Vol.186, pp. 32-37, doi:10.1016/j.sna.2011.12.055, 2012.

[12] H. Yokoyama, M. Sohgawa, T. Kanashima, T. Azuma, M. Okuyama, and H. Noma, "Fabrication and Noise Reduction of the Miniature Tactile Sensor Using Through-Silicon-Via Connection with Signal Amplifier," Jpn. J. Appl. Phys., Vol.52, No.6S, 06GL08, doi:10.7567/JJAP.52.06GL08, 2013.

[13] H. Yokoyama, T. Kanashima, M. Okuyama, T. Abe, H. Noma, T. Azuma, and M. Sohgawa, "Proximity and Tactile Sensing Using a Single MEMS Sensor with Photo- and Strain Sensitivities," IEEJ Trans. Sens. Micromachines, Vol.134, No.7, pp. 229-234, doi:10.1541/ieejsmas.134.229, 2014 (in Japanese).

[14] M. Sohgawa, A. Nozawa, H. Yokoyama, T. Kanashima, M. Okuyama, T. Abe, H. Noma, and M. Sohgawa, "Multimodal measurement of proximity and touch force by light- and strain-sensitive multifunctional MEMS sensor," Proc. of IEEE SENSORS 2014, pp. 1749-1752, doi:10.1109/ICSENS.2014.6985362, November 2014.

[15] K. Takahashi, T. Abe, M. Okuyama, H. Noma, and M. Sohgawa, "Surface Texture Characterization Using Optical and Tactile Combined Sensor," Sens. Mater., Vol.30, No.5, pp. 1091-1101, doi:10.18494/SAM.2018.1786, 2018.

[16] R. Araki, F. Suga, T. Abe, H. Noma, and M. Sohgawa, "Gripping control of delicate and flexible object by electromotive manipulator with proximity and tactile combo MEMS sensor," Proc. of Transducers 2017, pp. 1140-1143, doi:10.1109/TRANSDUCERS.2017.7994254, June 2017.

[17] R. Araki, T. Abe, H. Noma, and M. Sohgawa, "Electromotive Manipulator Control by Detection of Proximity, Contact, and Slipping Using MEMS Multiaxial Tactile Sensor," Electr. Eng. Japan, Vol.204, No.2, pp. 44-49, doi:10.1002/eej.23098, 2018.

[18] R. Araki, T. Abe, H. Noma, and M. Sohgawa, "Miniaturization and high-density arrangement of microcantilevers in proximity and tactile sensor for dexterous gripping control," Micromachines, Vol.9, No.6, 301, doi:10.3390/mi9060301, 2018.

[19] F. Suga, R. Araki, T. Abe, H. Noma, and M. Sohgawa, "Suppression of Deformation for Gripping Soft Objects Using Miniature Tactile Sensor with Hemisphere PDMS," Proc. of Asia-Pacific Conf. Transducers and Micro-Nano Tech. 2018, 123, June 2018.

Name:
Tomoya Fujihashi

Affiliation:
Graduate School of Science and Technology, Niigata University

Address:
8050 Ikarashi 2-no-cho, Nishi-ku, Niigata 950-2181, Japan

Brief Biographical History:

2018- Master's Student, Graduate School of Science and Technology, Niigata University

Name:
Fumitoshi Suga

Affiliation:
Graduate School of Science and Technology, Niigata University

Address:
8050 Ikarashi 2-no-cho, Nishi-ku, Niigata 950-2181, Japan
Brief Biographical History:
2017- Master's Student, Graduate School of Science and Technology, Niigata University
Main Works:
• R. Araki, F. Suga, T. Abe, H. Noma, and M. Sohgawa, "Gripping control of delicate and flexible object by electromotive manipulator with proximity and tactile combo MEMS sensor," Proc. of 19th Int. Conf. on Solid-State Sensors, Actuators and Microsystems (Transducers), pp. 1140-1143, June 2017.

Name:
Ryoma Araki

Affiliation:
Graduate School of Science and Technology, Niigata University

Address:
8050 Ikarashi 2-no-cho, Nishi-ku, Niigata 950-2181, Japan
Brief Biographical History:
2016- Master's Student, Graduate School of Science and Technology, Niigata University
Main Works:
• R. Araki, T. Abe, H. Noma, and M. Sohgawa, "Miniaturization and High-Density Arrangement of Microcantilevers in Proximity and Tactile Sensor for Dexterous Gripping Control," Micromachines, Vol.9, 301, June 2018.

Name:
Jyun Kido

Affiliation:
Graduate School of Science and Technology, Niigata University

Address:
8050 Ikarashi 2-no-cho, Nishi-ku, Niigata 950-2181, Japan
Brief Biographical History:
2018- Master's Student, Graduate School of Science and Technology, Niigata University
Main Works:
• J. Kido, Y. Abe, S. Sato, T. Abe, H. Noma, and M. Sohgawa, "Measurement by Tactile Sensor and FEM Analysis of Multi-layered Flexible Model for Skin Diagnosis," IEEJ Trans. on Sensors and Micromachines, Vol.139, pp. 149-154, 2019 (in Japanese).
Membership in Academic Societies:
• The Institute of Electrical Engineers of Japan (IEEJ)

Name:
Takashi Abe

Affiliation:
Graduate School of Science and Technology, Niigata University

Address:
8050 Ikarashi 2-no-cho, Nishi-ku, Niigata 950-2181, Japan
Brief Biographical History:
2003- Associate Professor, Tohoku University
2010- Professor, Niigata University
Main Works:
• H. Kutsuwada, S. Watanabe, M. Sohgawa, and T. Abe, "Fabrication of a true-Gaussian-shaped quartz crystal resonator," Sensors and Actuators A, Vol.260, pp. 58-61, 2017.
Membership in Academic Societies:
• The Institute of Electrical Engineers of Japan (IEEJ)
• The Japan Society of Mechanical Engineers (JSME)
• The Institute of Electrical and Electronics Engineers (IEEE)

Name:
Masayuki Sohgawa

Affiliation:
Graduate School of Science and Technology, Niigata University

Address:
8050 Ikarashi 2-no-cho, Nishi-ku, Niigata 950-2181, Japan
Brief Biographical History:
2007- Assistant Professor, Osaka University
2013- Assistant Professor, Niigata University
2016- Associate Professor, Niigata University
Main Works:
• T. Takahashi, S. Sato, T. Abe, and M. Sohgawa, "Tactile sensor using a microcantilever embedded in fluoroelastomer with resistance to cleaning and antiseptic solutions," Sensors and Actuators A, Vol.301, 111774, 2020.
Membership in Academic Societies:
• The Institute of Electrical Engineers of Japan (IEEJ)
• The Japan Society of Mechanical Engineers (JSME)
• The Institute of Electrical and Electronics Engineers (IEEE)